Wear 271 (2011) 1490–1496

Contents lists available at ScienceDirect

Wear

journal homepage: www.elsevier.com/locate/wear

Effect of low-temperature plasma carbonitriding on the fretting behaviour of 316LVM medical grade austenitic stainless steels

J. Liu[a,c], H. Dong[b], J. Buhagiar[b], C.F. Song[a], B.J. Yu[a], L.M. Qian[a,*], Z.R. Zhou[a]

[a] Tribology Research Institute, National Traction Power Laboratory, Southwest Jiaotong University, Chengdu 610031, China
[b] School of Metallurgy and Materials, The University of Birmingham, Birmingham B15 2TT, UK
[c] Special Equipment Supervision and Testing Institute, Tibet Bureau of Quality and Technical Supervision, Lhasa 850008, China

ARTICLE INFO

Article history:
Received 30 August 2010
Received in revised form
22 December 2010
Accepted 22 December 2010

Keywords:
Carbonitriding
Fretting wear
Medical grade austenitic stainless steels

ABSTRACT

An optimized low-temperature plasma carbonitriding process at 430 °C for 15 h was used to treat the surface of 316LVM medical grade austenitic stainless steel. By using a servo-hydraulic dynamic test machine, the fretting behaviour of both as-received and the surface-treated 316LVM plate samples against martensitic stainless steel balls was studied in the Ringer's solution at various displacement amplitudes. The experimental results demonstrate that the optimized low-temperature plasma surface treatment can produce a precipitate-free, C/N supersaturated S-phase layer. Such layer revealed a hardness of 5 times that of 316LVM substrate. The formation of S-phase can protect the 316LVM from corrosion in the Ringer's solution, and the hard surface-treated layer can significantly improve the fretting wear resistance of 316LVM material. When fretted in a mixed regime, a sharp drop of friction force was observed for untreated 316LVM after fretting for about 1000 cycles, which was mainly caused by the penetration of Ringer's solution into the contact area of the fretting pairs. As a comparison, no friction drop was observed through the fretting process on the surface-treated samples. Due to the high ratio of elastic modulus to hardness (E/H) of untreated sample, the main damage mechanism on untreated sample was adhesive and abrasive wear during the fretting process. However, because of the high hardness and low E/H ratio of the surface-treated sample, the main damage mechanism was mild abrasive wear. In conclusion, the low temperature plasma surface treatment can effectively improve the fretting wear properties of 316LVM stainless steel, which could pave the way to develop the high-performance, long-life body implants.

1. Introduction

Due to their low cost, proper mechanical behaviour and good formability, austenitic stainless steels have long been used as biomaterials, such as prosthetic bearing surfaces, orthodontic implants, bone fixation devices and cardiovascular devices [1]. However, the low wear resistance and the susceptibility to pitting corrosion in body fluids have limited their applications in the medical industry [2]. Combined improvement in corrosion and wear resistance is desirable for expanding their applications in long-life joint prostheses. Therefore, it is important to develop advanced surface treatment methods to improve the wear and corrosion resistance of austenitic stainless steels.

Based on the previous reports, low-temperature plasma carburizing treatment could produce a S-phase layer by introducing interstitials (N and C, or both) into an FCC structured substrate [3]. Such S-phase layer could reduce considerably the friction coefficient and improve the wear resistance of a Ni-free austenitic stainless steel in Ringer's solution. Dong [1] pointed out that the newly developed S-phase surface engineering technologies could provide stainless steels with a high surface hardness, good corrosion resistance, excellent tribological and tribochemical properties and outstanding fatigue properties for the design of demanding components. Rybiak et al. [4] noted that when tested above a threshold temperature of 220 °C, the friction coefficient and wear rate of stainless steels would decrease. The severe adhesive wear played a dominated role at low temperatures, whereas a third body abrasive process involving the formation of a compliant glaze layer structure took place at high ones. Low temperature surface treatment could increase the surface hardness and provide both low friction coefficient and excellent wear resistance against tungsten carbide balls [5]. It has been reported that the abrasive and adhesive wear resistance of austenitic stainless can be greatly improved after plasma nitriding, which was critical to the tribological application of the surface modification technique [6,7]. Nosei et al. [8] reported that ion nitriding of steels was a well known process mainly for surface hardening to improve their tribological properties and corrosion resistance. Liu et al. [9] demonstrated that low temperature

* Corresponding author. Tel.: +86 28 87600687; fax: +86 28 87603142.
E-mail address: linmao@swjtu.edu.cn (L.M. Qian).

0043-1648/$ – see front matter © 2011 Elsevier B.V. All rights reserved.
doi:10.1016/j.wear.2010.12.017

Table 1
Composition of 316LVM and AISI 440C steels, wt%.

Composition	C	Si	Mn	P	S	Cr	Ni	Mo	Cu	N	Fe
316LVM steel	0.019	0.5	1.87	0.025	0.003	17.43	13.75	2.72	0.1	0.084	bal.
AISI440C steel	1.1	0.8	0.6	–	–	17	–	0.6	–	–	bal.

plasma surface treatments, carbonitriding at 430 °C, carburizing at 500 °C and nitriding at 430 °C, could enhance the anti-corrosion and anti-wear properties of 316LVM stainless steel to some extent, and the first one was the best among these surface treatment methods. Despite all that, the fretting behaviour of the S-phase layer formed on 316LVM medical grade austenitic steels has not been well addressed.

In this paper, an optimized low-temperature plasma carbonitriding process at 430 °C for 15 h was used to treat the surface of 316LVM medical grade austenitic stainless steel. With a servo-hydraulic dynamic test machine, the fretting behaviour of both as-received and surface-treated 316LVM plate samples against martensitic stainless steel balls was studied in the Ringer's solution at various displacement amplitudes. A series of analyses, such as the frictional logs, the surface morphology and the cross-sectional profiling of the wear scars, were carried out. The wear mechanisms involved in the fretting process of untreated and surface-treated 316LVM sample were discussed.

2. Materials and testing methods

The material used in this study was 316LVM medical grade austenitic stainless steel. Block samples of $25 \times 6 \times 6\,mm^3$ were cut from the bar. The flat surfaces of the block samples were firstly wet ground using silicon carbide paper from 120 down to 1200 grit, and then polished using 6 μm and 1 μm diamond suspension in turn. Finally, the roughness (R_a) on the surface of samples was measured as 0.06–0.08 μm. Low temperature plasma carbonitriding was carried out at 430 °C for 15 h in a gas mixture containing 1.5% CH_4 and 98.5% H_2 at a constant pressure of 400 Pa in a 60 kW Klöckner dc plasma unit. After the treatment, a surface layer with a thickness of 25 μm was formed. AISI 440C stainless steel balls of 40 ± 0.1 mm in diameter were selected as the counterpart, which moved horizontally against the stationary plate specimen. The component elements of 316LVM and AISI 440C steels were listed in Table 1. The phase constituents in the as-received and plasma-treated surfaces were analyzed with an X'Pert Philips X-Radiation diffractometer (XRD) using Cu-Kα radiation (λ = 0.15419 nm). As shown in Fig. 1, compared to the untreated material, the peaks of surface-treated 316LVM samples were shifted to lower angles, which was the characteristic signature of the S-phase layer. This indicates that a C/N supersaturated S-phase layer has been produced after the treatments [10].

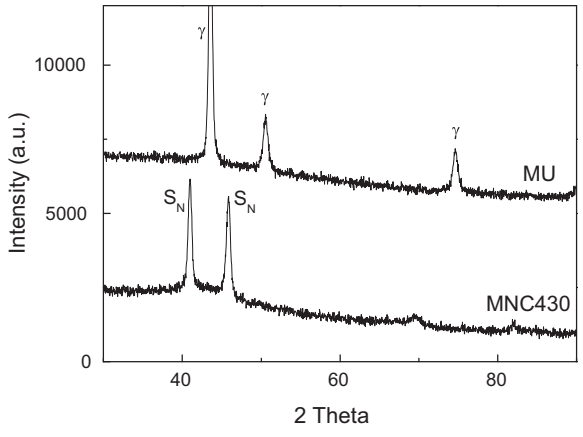

Fig. 1. XRD charts of untreated (MU) and surface-treated (MNC430) 316LVM stainless steel.

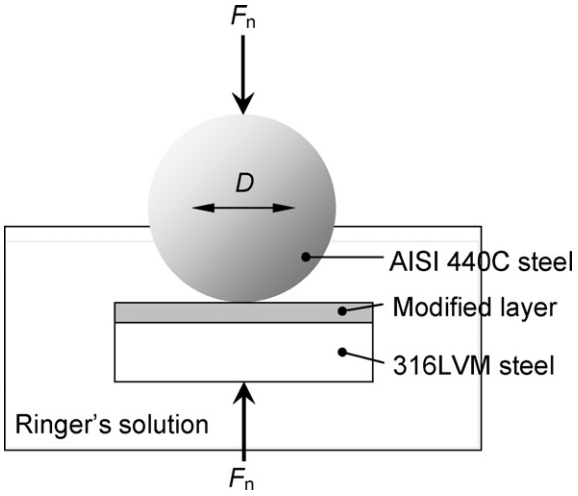

Fig. 2. The schematic diagram of the horizontal servo-hydraulic fretting apparatus. During fretting tests, the upper AISI 440C steel ball moved horizontally with a displacement amplitude of D under a normal load of F_n.

With a nanoindenter (Nano-Hardness/Scratch Tester, CSM, Switzerland), the nanoindentation hardness H and elastic modulus E of untreated (MU) and surface-treated (MNC430) 316LVM sample were measured. The load capacity of the S-phase was characterized by the scratch tests with the same instrument.

All the fretting tests were conducted using a horizontal servo-hydraulic fretting apparatus (DS20 PLINT, France) under a normal load of 100 N at a frequency of 5 Hz in Ringer's solution. The schematic diagram of the horizontal servo-hydraulic fretting apparatus was shown in Fig. 2. During fretting tests, the upper AISI 440C steel ball moved horizontally with a displacement amplitude of D under a normal load of F_n. The number of fretting cycles was 1500–10,000. The displacement amplitude D was ranged from 3 μm to 40 μm. The tangential force F_t and the number of cycles N were recorded by the test machine. All the fretting tests were carried out in atmosphere with the temperature of 15–20 °C and relative humidity of 40–50%. Under each condition, the fretting test was repeated at least 3 times to ensure the repetition of data. After the fretting tests, the morphologies of the wear scars were characterized by an optical microscope and a scanning electron microscope (SEM, Qunta200, FEI, Holland), and the chemical composition of the materials in the wear scars was analyzed by an energy dispersive X-ray detector (EDX, INCA PENTAFET X3, Oxford Instruments Technology, England).

3. Experimental results

3.1. Surface mechanical properties

The nano-mechanical properties in terms of hardness H and elastic modulus E of the plasma treated and untreated material were probed using a nanoindentation machine and the results were summarized in Table 2. It can be seen that the hardness and elastic modulus of 316LVM was improved by 393% and 24% respectively

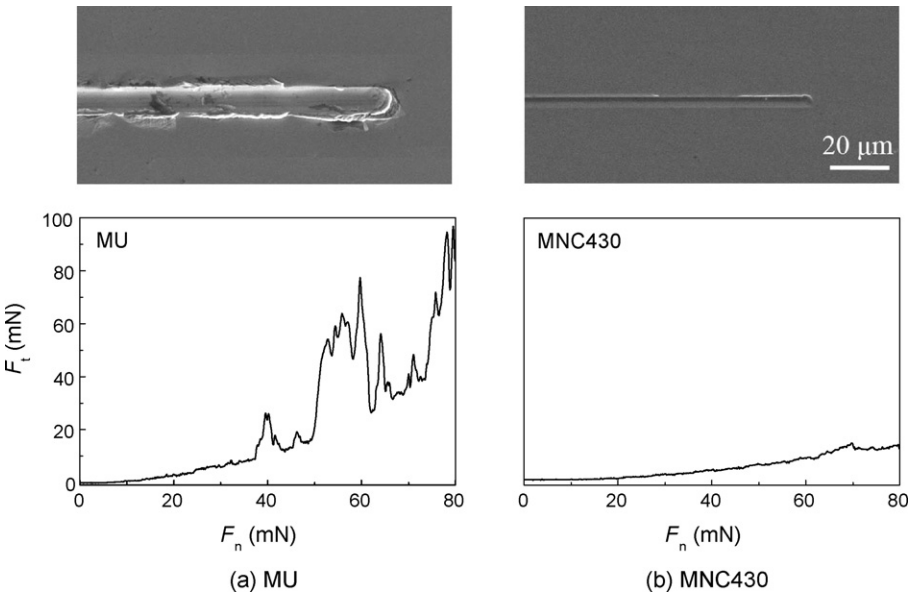

Fig. 3. The tangential force F_t versus normal load F_n curves and the SEM images of the scratch scars on untreated (MU) and surface-treated (MNC430) 316LVM stainless steel.

Table 2
Nano-mechanical properties of untreated and surface-treated samples.

Sample	H (GPa)	E (GPa)	E/H
Untreated (MU)	2.7	170.5	63.1
Treated (MNC430)	13.3	210.7	15.8

and the E/H ratio was reduced by 75% accordingly following the plasma surface treatment. It was reported that nitrogen ion implantation processes can enhance the surface hardness of 316LVM by 20–86% only [11]. Clearly, plasma surface treatment is much more effective than ion implantation in hardening austenitic stainless steel.

The load capacity of the S-phase was characterized by scratch tests with a Nano-Scratch Tester. As shown in Fig. 3, with the increase in the normal load, the tangential force of the scratch on untreated (MU) sample fluctuated greatly, while that on surface-treated (MNC430) sample showed a slow and smooth increase. As the load increased to 80 mN, the tangential force on MU sample reached 100 mN, which was about 8 times that on MNC430 sample. As a result, the scratch formed in MU sample was much deeper and wider than that formed in MNC430, as evidenced by the SEM images in Fig. 3. The results demonstrate that the surface treatment can effectively improve the load capacity of MU sample through the formation of S-phase.

3.2. Effect of surface treatment on fretting regimes

Fig. 4 shows the typical frictional logs (F_t–d–N curves) of the as-received and surface treated 316LVM against AISI 440C stainless steel balls under various values of displacement amplitude D in the Ringer's solution. When the fretting occurred between the MU sample and stainless steel ball (MU/ball pairs), three typical fretting regimes could be determined from the frictional logs under various values of D. When the values of D were below 7 μm, the tangential force versus displacement (or F_t–d) curves were in the quasi-closed shape, indicating a partial slip regime. When the values of D were above 20 μm, all the F_t–d curves were open and finally in a parallelogram shape, which was the characteristic of the gross slip regime. Finally, when the values of D varied between 7 μm and 20 μm, the curves were characterized by elliptic and parallelogram shape, showing the behaviour of the mixed fretting regime

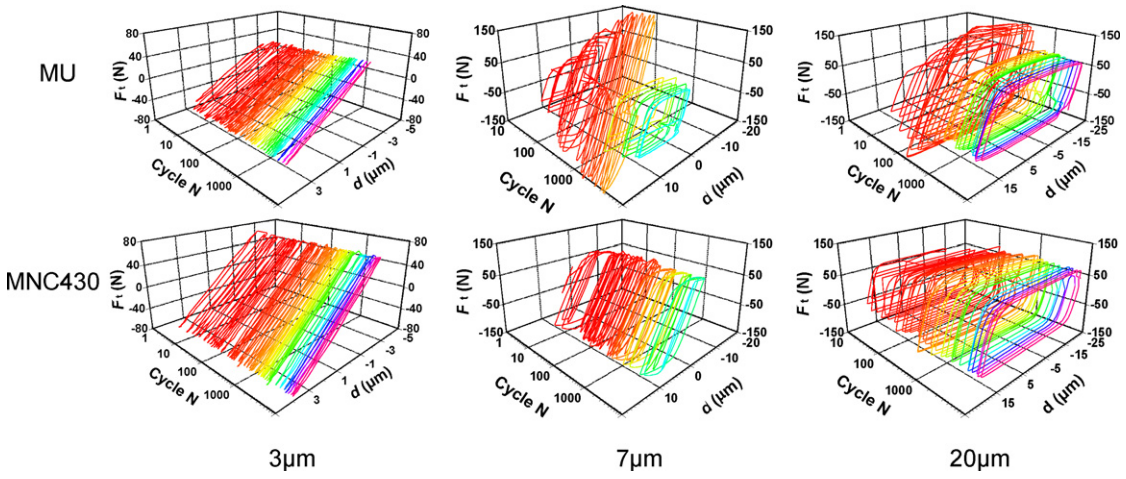

Fig. 4. F_t–d–N curves of untreated (MU) and surface-treated (MNC430) 316LVM stainless steel under various fretting displacement amplitudes. The applied normal load is 100 N.

Table 3
Effect of surface treatment on the fretting regimes of 316LVM stainless steel against AISI 440C stainless steel balls.

Fretting regimes	Partial slip regime	Mixed slip regime	Gross slip regime
MU/ball pairs	$D < 7\,\mu m$	$D = 7–20\,\mu m$	$D \geq 20\,\mu m$
MNC430/ball pairs	$D < 15\,\mu m$	–	$D \geq 15\,\mu m$

[12]. However, the surface treatment showed a strong effect on the fretting regimes. As shown in Fig. 4, the surface treated layers could extend the gross slip regime of the MU/ball pairs to the relatively smaller displacement amplitude 15 μm. For $D \leq 15\,\mu m$, no mixed regime was identified and the MNC430 against AISI 440C (MNC430/ball) pairs ran in partial slip regime. The fretting regimes of two pairs were summarized in Table 3.

The variation of the tangential force F_t with the increase in the number of fretting cycles N was also an important indicator to the fretting kinetic behaviour. The F_t–N curves of the fretting of MU/ball and MNC430/ball pairs under various values of D were plotted in Fig. 5. As shown in Fig. 5a, in the partial slip regime of MU/ball pairs ($D = 3\,\mu m$), the tangential forces reached its stable value in the 40th cycle after the initial increase. However, when the fretting of MU/ball pairs ran in mixed regime ($D = 7\,\mu m$ or $10\,\mu m$) and gross slip regime ($D = 20\,\mu m$), the tangential forces increased rapidly in the first 100–1000 cycles and then dropped quickly to their stable values. During the initial fretting cycles, surface asperities on the contact area were worn down gradually, resulting in the increase of the real contact area. Since the friction force is proportional to the contact area, the friction coefficient on MU and MNC430 undergoes the similar increasing trend during the initial cycles [13,14]. It was also noted that when the fretting of MU/ball pairs ran under a larger value of D, the tangential forces started to decrease earlier and the stable values were higher. However, the F_t–N curves of the fretting of MNC430/ball pairs were much different from those of MU/ball pairs. As shown in Fig. 5b, either in the partial slip regime ($D = 3–10\,\mu m$) or in the gross slip regime ($D = 20\,\mu m$), no drop of tangential force was observed and the tangential force increased to a constant value after 100–500 fretting cycles.

3.3. Effect of surface treatment on fretting wear properties

To investigate the fretting wear mechanism of as-received and surface treated 316LVM, the morphologies of wear scars were examined by an optical microscope and the cross-sectional profiles were measured by a stylus profilometer. As shown in Fig. 6, when the fretting ran in partial slip regime ($D = 3\,\mu m$), all the wear scars of MU and MNC430 samples could be divided into two parts, the stick zone in the center and the micro-slip zone at the edge. As the fretting of MU/ball pairs ran in mixed regime ($D = 7\,\mu m$), the entire wear scar area on MU surface was rough and some cracks were formed around the edges. However, under the same fretting conditions, the wear scar on MNC430 surface still revealed the characteristics of partial slip regime, namely as an inner stick area and an outer micro-slip area. Finally, when the fretting of these two pairs ran in gross slip regime ($D = 20\,\mu m$), the main wear mechanism of MU/ball pairs was adhesion, while MNC430/ball pairs underwent mild abrasion.

Fig. 7 plotted the average wear depth h of the wear scars on MU and MNC430 samples after fretting for 10,000 cycles as a function of D. As the fretting ran in partial slip regime ($D = 3\,\mu m$), the h was 0.7 μm on MU and 0.6 μm on MNC430 surfaces. For $D = 7\,\mu m$, the MU/ball pairs ran in mixed regime and the h on MU was 4.7 μm. However, since the MNC430/ball pairs still ran in partial slip regime, the h on MNC430 was 0.8 μm, which was only 18% of that on MU. Finally, when the fretting ran in gross slip regime ($D = 20\,\mu m$), the h was 2.7 μm on MU and 0.6 μm on MNC430 surface. Obviously, low temperature plasma surface treatment has effectively improved the fretting wear properties of 316LVM stainless steel.

3.4. Effect of surface treatment on fretting corrosion behaviour

The EDX detection may provide information to some extent on the corrosion resistance of sample in the fretting test [15]. After fretting in Ringer's solution for 10,000 cycles, the EDX spectrum on the wear scars of MU and MNC430 samples were detected. As shown in Fig. 8, high oxygen and chlorine peaks appeared in the center of the wear scar of MU sample but they could not be detected in the wear scar of MNC430 sample. The enrichment of the chlorine on MU was due to the penetration of the Ringer's solution. It was noted that the MU sample was worn and corroded heavily in the solution during the fretting. Therefore, the carbonitrided sample exhibited better anti-corrosion behaviour than untreated material. It can be speculated that the formation of S-phase on the surface layer played an important role in the protection of the 316LVM substrate from corrosion in the Ringer's solution. Even though, the effect of surface treatment on the corrosion resistance of 316LVM medical grade austenitic stainless steel under fretting conditions should be investigated on-line by the electrochemical method in future.

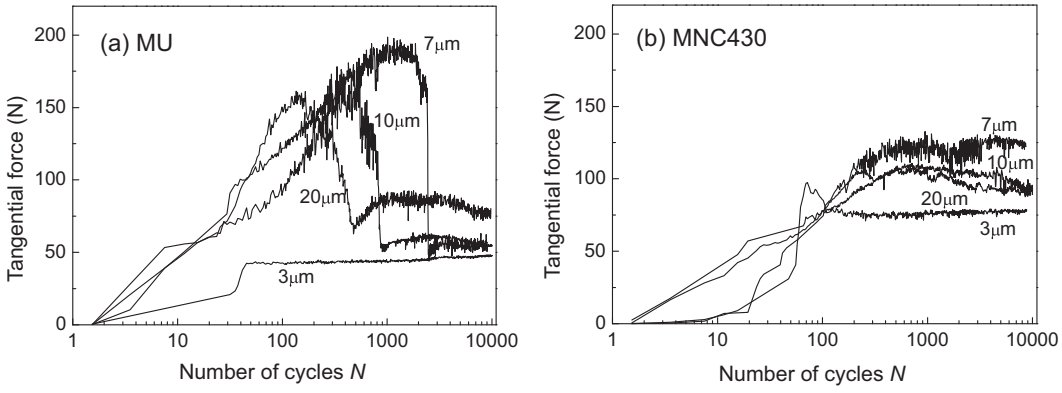

Fig. 5. The tangential force versus the number of fretting cycles curves of as-received and surface treated 316LVM against AISI 440C steel ball under various displacement amplitudes. The applied normal load is 100 N.

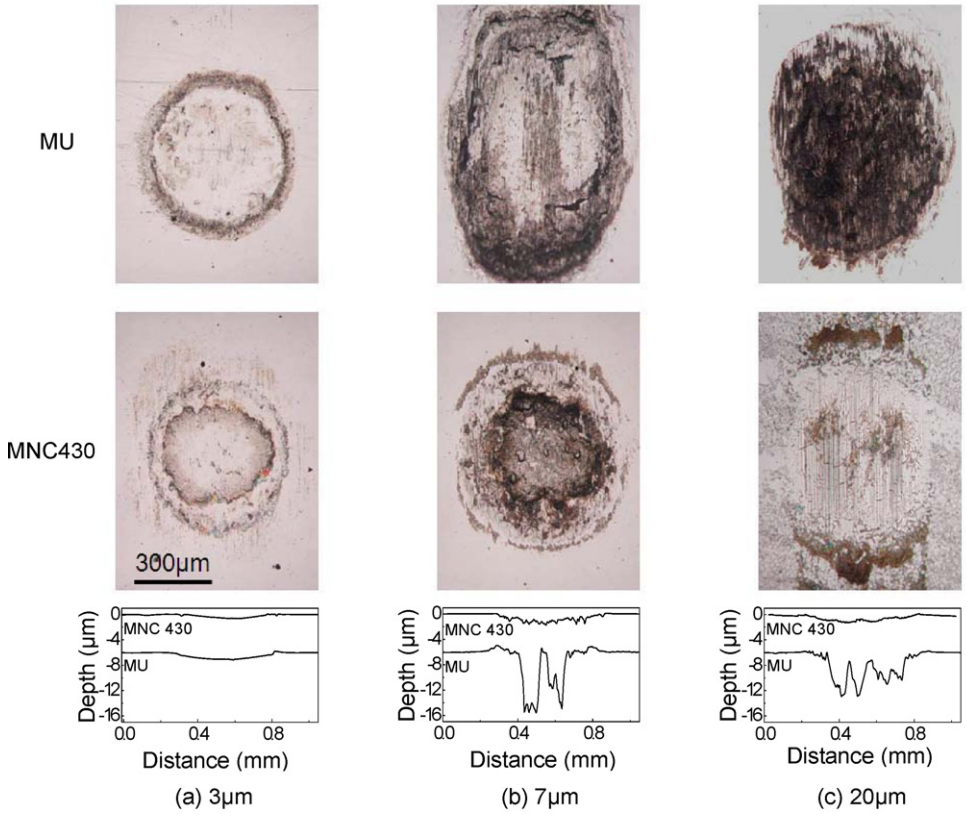

Fig. 6. The optical morphology of the wear scars on untreated (MU) and surface-treated (MNC430) 316LVM stainless steel after fretting for 10,000 cycles under various displacement amplitudes. The applied normal load is 100 N.

4. Discussion

It can be seen in Fig. 5 that when the fretting of MU/ball pairs ran in the mixed regime, the tangential forces decreased sharply to stable values after the initial increase. However, such drop of tangential forces was not observed in the fretting of MNC430/ball pairs. To understand the reason for the drop of the tangential forces, the cross sections of fretting scars were examined by a SEM. Fig. 9 showed the SEM images of the panorama, details and cross section of the wear scars on MU and MNC430 surfaces after the fretting of these two pairs under $D = 7\,\mu m$. After 10,000 fretting cycles, the generation of cracks was observed on MU sample, as shown in Fig. 9a. However, the generation of cracks was effectively prevented by the plasma surface treatment, as shown in Fig. 9c. Even after 1584 fretting cycles, where the tangential force of MU/ball pairs began to drop, a clear crack was formed on MU samples.

It is reported that the generation of cracks can lead to the fluctuation of the tangential force [16]. But the penetration of the lubrication solution into the contact area was also been found responsible for the drop of tangential force [17]. To verify which one was the main reason, the fretting of MU/ball pairs was conducted under both dry and lubrication conditions. As shown in Fig. 10a, when the fretting of MU/ball pairs ran in lubricated condition, the tangential force decreased sharply from the peak value of 140 N to

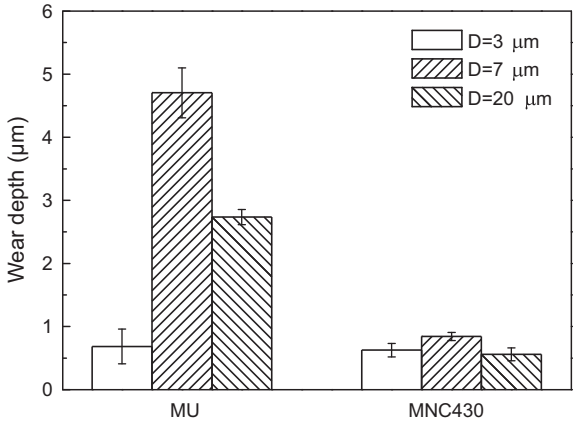

Fig. 7. The average wear depth of untreated (MU) and surface-treated (MNC430) 316LVM stainless steel after fretting for 10,000 cycles under various displacement amplitudes. The applied normal load is 100 N.

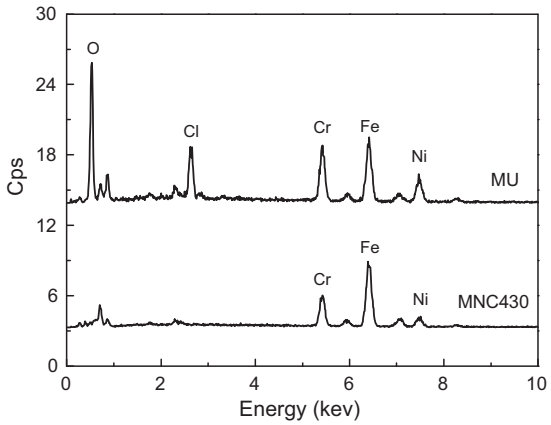

Fig. 8. The EDX spectrum on the center of the fretting wear scars of MU and MNC430 samples.

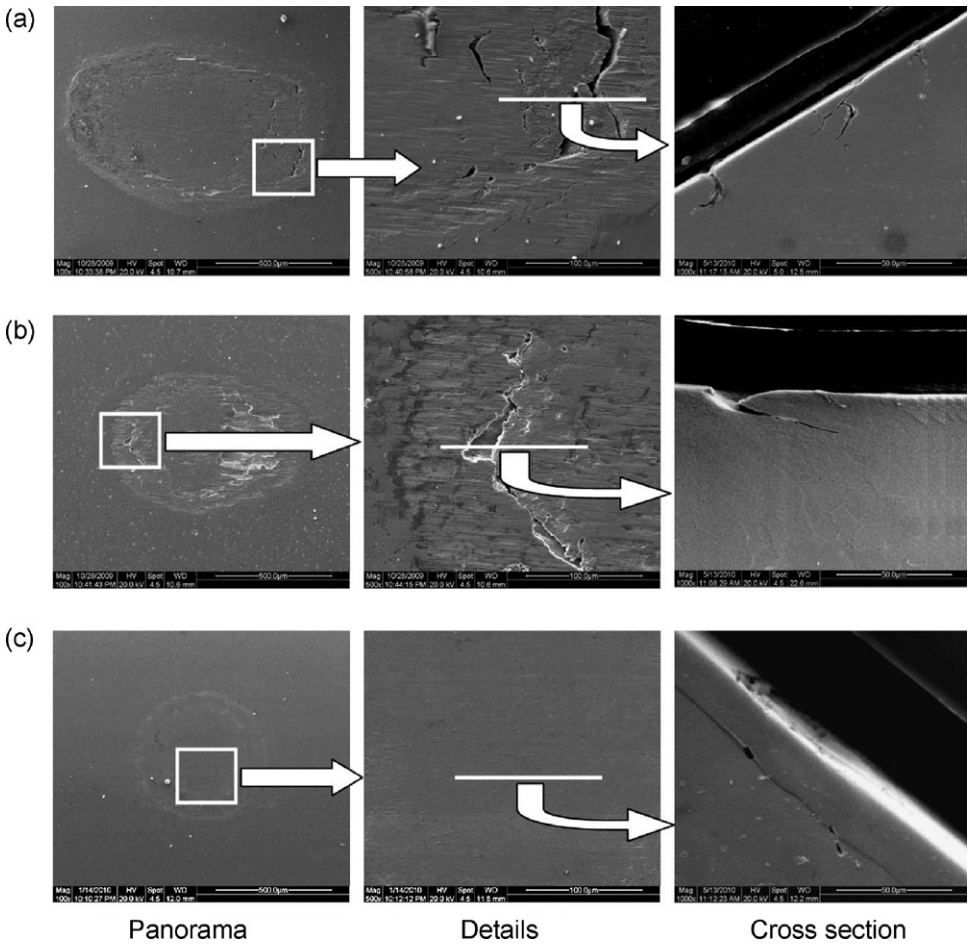

Fig. 9. The SEM images of the panorama, detail and cross section of the wear scars under $D = 7\ \mu m$. (a) Untreated sample and $N = 10{,}000$ cycles; (b) untreated sample and $N = 1584$ cycles; (c) surface-treated sample and $N = 10{,}000$ cycles.

the stable value of 40 N around 1000 cycles, but no cracks were observed on the wear scar. However, when the fretting of MU/ball pairs ran in dry condition, no rapid drop in the tangential force was recorded and no cracks were generated on the wear scar of MU sample. When the fretting runs under dry condition, the creation of debris can lead to a three-body contact on the entire surface

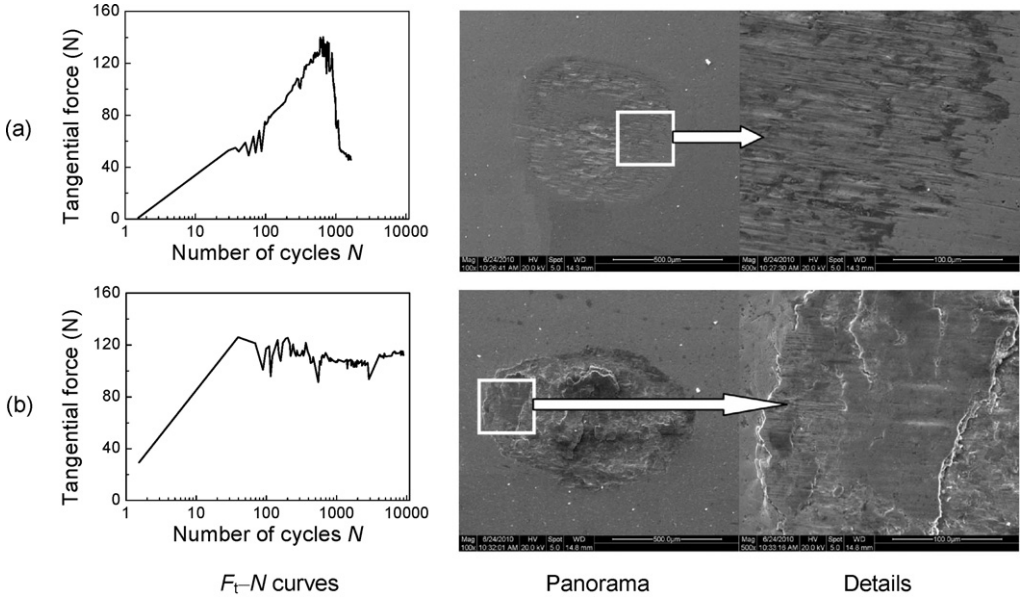

Fig. 10. The F_t–N curves and SEM images of the wear scars after fretting under $D = 7\ \mu m$. (a) after 1636 fretting cycles in Ringer's solution; (b) after 10,000 fretting cycles under dry condition. The applied normal load is 100 N.

and induce the decrease of tangential force [13]. Therefore, even though the generation of cracks might decrease the tangential force to some extent, the sharp drop of tangential force of MU/ball pairs in Ringer's solution was mainly induced by the penetration of solution into the contact area.

During the fretting process of MU/ball pairs in Ringer's solution, since the ratio of elastic modulus to hardness (E/H) for MU sample was as high as 63.1 (Table 2), strong adhesion wear can be detected from the friction loops and wear scars (Figs. 4 and 6) [18]. Hence, the solution was difficult to penetrate into the contact surface in the initial hundreds of fretting cycles. After hundreds of fretting cycles, the contact surface might be damaged and the abrasive debris was generated as the three-body. Under this condition, the solution might penetrate into the contact area and a rapid drop in the tangential force occurred [17]. The penetration of the solution was also depended on the displacement amplitude D. With the increase in the values of D, the penetration was easy to occur and the number of turning point cycle (at which cycle the tangential force began to drop) was reduced [17]. As shown in Figs. 4 and 5, with the increase in the values of D from 7 μm to 20 μm, the number of the turning point cycle decreased from 2000 to 200. Compared to the high E/H ratio of MU sample, the E/H ratio of MNC430 was only 15.8. Thus, both the plastic deformation and the adhesion junction in the contact area were largely reduced, consequently resulting in the decrease of adhesive wear. Therefore, no drop of tangential force was observed and the solution might penetrate into the contact area in the first several cycles.

In summary, the rapid drop of the tangential force of MU/ball pairs was mainly induced by the penetration of the Ringer's solution into the contact area. The main wear mechanism of the MU/ball pairs was adhesion and abrasion. The surface treatment could strongly improve the wear behaviour of 316LVM substrate.

5. Conclusions

An optimized low-temperature plasma carbonitriding process at 430 °C for 15 h was used to treat the surface of 316LVM medical grade austenitic stainless steel. With a servo-hydraulic dynamic test machine, the fretting behaviours of both as-received and surface-treated samples against martensitic stainless steel balls were studied in the Ringer's solution at various displacement amplitudes. Based on the experimental results and discussion, the main conclusions can be summarized as follows.

(1) After low temperature plasma carbonitriding treatment, the surface hardness of 316LVM has been improved by 5 times and the elastic modulus increased by 24%. The surface-treated layer can not only expand the gross slip regime of MU/ball pairs to low displacement amplitude, but also effectively improve the corrosion and wear behaviour of 316LVM substrate.
(2) When the fretting of MU/ball pairs ran in mixed regime, a sharp drop of tangential force was observed after the initial increase, which was mainly induced by the penetration of Ringer's solution into the contact area of fretting pairs. However, such drop could be largely limited by the surface treatment of MU sample.
(3) Due to the high value of E/H ratio of untreated sample, the main damage mechanism of MU/ball pairs was adhesive and abrasive wear during the fretting process. However, because of the high hardness and low E/H ratio of the surface-treated sample, the main wear mechanism of MNC430/ball pairs was mild abrasion.

Acknowledgements

The authors are grateful for the financial support from the National Basic Research Program (2011CB707604) and the Natural Science Foundation of China (90923017, 50625515 and 50821063).

References

[1] H. Dong, S-phase surface engineering of Fe–Cr, Co–Cr and Ni–Cr alloys, Int. Mater. Rev. 55 (2010) 65–98.
[2] K.L. Hsu, T.M. Ahn, D.A. Rigney, Friction, wear and microstructure of unlubricated austenitic stainless steels, Wear 60 (1980) 13–37.
[3] J Buhagiar, L.M. Qian, H. Dong, Surface property enhancement of Ni-free medical grade austenitic stainless steel by low-temperature plasma carburizing, Surf. Coat. Technol. 205 (2010) 388–395.
[4] R. Rybiak, S. Fouvry, B. Bonnet, Fretting wear of stainless steels under variable temperature conditions: introduction of a 'composite' wear law, Wear 268 (2010) 413–423.
[5] X. Nie, C. Tsotsos, A. Wilson, A.L. Yerokhin, A. Leyland, A. Matthews, Characteristics of a plasma electrolytic nitrocarburising treatment for stainless steels, Surf. Coat. Technol. 139 (2001) 135–142.
[6] T. Zheng, Y.H. Qiang, N. Zhang, Study on CN ion implantation austenitic stainless steel, Hot Working Technol. 2 (2005) 16–17.
[7] Y.Q. Xia, S.J. Wang, F. Zhou, H.Z. Wang, Y.M. Lin, T. Xu, Tribological properties of plasma nitrided stainless steel against SAE52100 steel under ionic liquid lubrication condition, Tribol. Int. 39 (2006) 635–640.
[8] L. Nosei, S. Farina, M. Avalos, L. Nachez, B.J. Gomez, J. Feugeas, Corrosion behavior of ion nitrided AISI 316L stainless steel, Thin Solid Films 516 (2008) 1044–1050.
[9] J. Liu, L.M. Qian, H.S. Dong, J. Buhagiar, Effect of surface treatment on the fretting wear behavior of medical grade austenitic stainless steels, Tribology 29 (5) (2009) 399–404.
[10] J. Buhagiar, H. Dong, S-phase in stainless steels: an overview, Surf. Modif. Technol. (2008) 509–518.
[11] N. Zhang, Y.H. Qiang, C.H. Zhang, J.N. Niu, F.X. Wang, Study on surface performance of biomedical metallic materials implanted by nitrogen ion, Mater. Heat Treat. 36 (4) (2007) 52–57.
[12] Z.R. Zhou, L. Vincent, Mixed fretting regime, Wear 181–183 (1995) 531–538.
[13] R.W. Carpick, D.F. Ogletree, M. Salmeron, A general equation for fitting contact area and friction vs load measurements, J. Colloid Interface Sci. 211 (1999) 395–400.
[14] P. Blanchard, C. Colombie, V. Pellerin, S. Fayeulle, L. Vincent, Material effects in fretting wear: application to iron, titanium, and aluminium alloys, Metall. Mater. Trans. A 22 (1991) 1535–1544.
[15] H. Dong, P.Y. Qi, X.Y. Li, R.J. Llewellyn, Improving the erosion–corrosion resistance of AISI 316 austenitic stainless steel by low-temperature plasma surface alloying with N and C, Mater. Sci. Eng. A – Struct. 431 (2006) 137–145.
[16] L. Lin, G.S. Blackman, R.R. Matheson, Quantitative characterization of scratch and mar behavior of polymer coatings, Mater. Sci. Eng. A317 (2001) 163–170.
[17] Q.Y. Liu, Z.R. Zhou, Effect of displacement amplitude in oil-lubricated fretting, Wear 239 (2000) 237–243.
[18] B. Casas, et al., Adhesion and abrasive wear resistance of TiN deposited on electrical discharge machined WC–Co cemented carbides, Wear 265 (2008) 490–496.